SAGE CRISP PUBLICATIONS DIRECTORY

Authors:-

Kusakabe, O., Maeda, Y., Ohuchi, M. and Hagiwara, T.

ATTEMPTS AT CENTRIFUGAL AND NUMERICAL SIMULATION OF A LARGE SCALE IN SITU LOADING ON A GRANULAR MATERIAL,

Publication:-

PREDICTIVE SOIL MECHANICS
PROCEEDINGS OF THE WROTH MEMORIAL SYMPOSIUM, ST CATHERINE'S COLLEGE, OXFORD
pp 404 - 420

Year of Publication:-

1992

CRISP

Attempts at centrifugal and numerical simulations of a large-scale in situ loading test on a granular material

O. KUSAKABE, Hiroshima University, Y. MAEDA, Japan Highway Public Cooperation, M. OHUCHI, Shiraishi, Co. Ltd, and T. HAGIWARA, Gunma University, Japan

This paper describes a large-scale in situ loading test on a scoria, a granular material produced by volcanic eruptions, conducted in a pneumatic caisson. Presented also are test results on undisturbed scoria samples procured from the loading test site. For the loading test, two types of simulation were attempted: centrifugal simulation using undisturbed samples and FEM simulation of the CRISP package using the element test data. It was found that centrifugal simulations using undisturbed samples predicted the yield load, and elastic deformations close to the prototypes, but clear slip lines were not developed and settlements at yield load were much larger than those in prototype. It was inferred that the observations may be partly due to particle size effect. Difficulty in the selection of soil parameters in the FEM analysis was encountered and uncertainty in the determination of K_0 values for very high overconsolidation ratios was recognized.

Introduction

Two types of modelling are available for geotechnical problems: physical modelling and numerical modelling. The validation of these modellings requires well documented prototype behaviour, with which the effectiveness of the modellings can be directly compared. This study focuses on two particular modelling techniques: the centrifuge test and CRISP FEM programme, both of which have been developed at Cambridge University.

Direct comparisons between centrifuge modelling and prototype behaviour have been relatively rare in number, compared with FEM versus prototype comparisons. For clays, Lyndon and Schofield (1970, 1978) reported successful centrifuge simulations of failures on natural slopes of London clay and Lodalen landslide using undisturbed block samples. Basset and Horner (1979) also attempted such direct comparisons with prototypes of clay foundations.

 Predictive soil mechanics. Thomas Telford, London, 1993

Well documented field data are scarce. Detailed information on soil element behaviour and boundary conditions are needed for proper comparison with prediction. Since these details can be determined for well controlled centrifuge tests, this had led to such tests being regarded as prototypes. Many centrifuge modellers have attempted direct comparisons between centrifuge tests of this type and FEM predictions using the CRISP package (Britto and Gunn, 1987). Works by Basset et al. (1981), Kimura et al. (1984), Almeida et al. (1984), Davies and Parry (1985) are good examples. All these works have dealt with the problems of clay foundations and they seem to share the view that FEM analysis using the CRISP package can predict centrifuge results with acceptable accuracy. Quite recently Indraratna et al. (1992) utilized the CRISP package to analyse a field test embankment behaviour on a clay foundation.

In contrast, for granular materials there still exists scepticism about the accuracy of predictions by centrifuge tests and about the CRISP analysis. Only limited information is available for us to reach any conclusion about the validity of centrifuge modelling and FEM predictions compared with prototype behaviour. Fujii et al. (1988) compared large-scale in situ field loading tests of shallow foundations on a pumice flow deposit called Shirasu with centrifuge tests using undisturbed samples. They concluded that the centrifuge tests could predict ultimate bearing capacities fairly well, but overestimated settlement behaviour by a factor of 2 to 3. They inferred that the difference in settlement behaviour might have stemmed from sampling disturbance.

Recently Tatsuoka et al. (1991) conducted a direct comparison of loading tests of shallow footings between a 1G model and corresponding centrifuge tests using dry Toyoura sand. They claimed that the particle size effect cannot be ignored for centrifuge simulations for granular materials. Bolton and Lau (1988) performed centrifuge tests on particle size modelling, from which they stated that the particle size modelling may cause another complication due to the fact that smaller particles have higher crushing pressures.

This paper describes a large-scale in situ loading test on a scoria, a granular material produced by volcanic eruptions, conducted in a pneumatic caisson. Presented also are test results on undisturbed scoria samples procured from the loading test site. For this particular loading test, two types of simulation were attempted: centrifugal simulation using undisturbed samples and FEM simulation of the CRISP package using the element test data. Direct comparisons with the prototype are presented in terms of load–settlement curves, failure mechanism and characteristics of particle crushing.

It should be mentioned here that the scoria is very different from the Kaolin and the standard sand generally used in simulations. While the

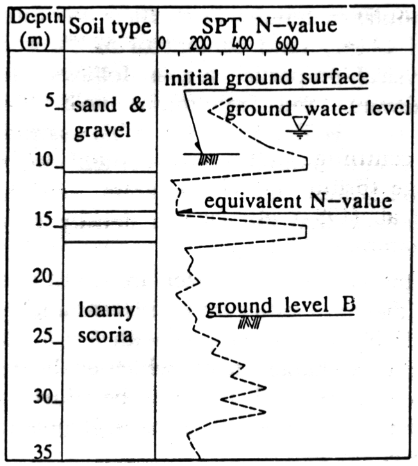

Fig. 1. Soil profile and elevation of loading test

result of this study is that the simulations are of 'predictive' value, nevertheless care should always be exercised in extending modelling techniques to new materials.

In situ loading tests

Test site and soil properties

A series of loading tests was conducted in the base chamber of a caisson under construction, of dimensions 16 m in diameter, and 23 m in height when completed. Figure 1 presents the soil profile of the test site with the level of ground water, consisting of a thick layer of dark brown scoria mixed with loam from 16.8 m below the ground surface and overlying layers of gravel and sandy deposits. The loading test selected for the direct comparison in this study was the one conducted at 14 m below the ground level, called B ground hereafter. The SPT-N values of the scoria layer are over 70 at the B ground.

The scoria belongs to the eruptions of Old Hakone Volcano deposited in the Quaternary period and has high angularity and numerous small voids. Prior to the loading test, undisturbed samples were manually cut from the test ground level in the form of blocks of 0.4 m length, 0.3 m width and 0.3 m height. These block samples were used for both element and centrifuge tests.

The soil test programme included physical tests, isotropic compression tests and triaxial compression tests under drained conditions (CID test). The grain size distribution curve of the B ground level showed that the scoria is a granular material with coefficient of uniformity U_c of 4.69, gravel content of 40.0%, sand content of 57.7% and fines content of 2.3%. Other physical properties are as follows: the specific gravity $G_s = 2.85$, maximum and minimum void ratios $e_{max} = 1.74$, $e_{min} = 1.17$, in situ void ratio $e_0 = 1.05$, saturated unit weight $\gamma_{sat} = 18.6\,kN/m^3$, and natural water content $W_n = 37.0\%$, average grain size $D_{50} = 1.57\,mm$, maximum grain size $D_{max} = 19.0\,mm$. It should be emphasized that the relative density in situ is as large as 121%.

The blocks of the scoria were frozen in unsaturated conditions and then cut out by a diamond cutter from different angles (δ) relative to the horizontal plane to obtain the samples with $\delta = 0, 30, 60, 90, -60$ and -30 degrees for the mechanical tests, which enabled us to examine the degree of anisotropy of the soil. It should be added here that the effect of freezing and thawing was found to be negligible in the stress–strain curves (Kusakabe et al., 1991).

Stress–strain curves of the CID triaxial tests for various confined pressures are shown in Fig. 2 for the cases of $\delta = 90°$. In common with cemented sands, the soil behaviour changes from that of a dilatant brittle material to that of a plastic material showing volume reduction during shearing as the confining pressure increases; as if the scoria behaves like a loose sand or a normally consolidated clay under high pressures. By defining the failure state at the axial strain of 15%, when the peak value was not observed, the failure envelopes of Mohr's Circles at failure as well as at residual states can be shown in Fig. 3, from which $c_d = 191\,kPa$, $\phi_d = 33.3°$, and $c_r = 76\,kPa$, $\phi_r = 33.9°$ were obtained. It is clear that the scoria is cemented and structured.

The data of $(\sigma_1' - \sigma_3')_f/\sigma_3'$ at failure for the samples with different angles

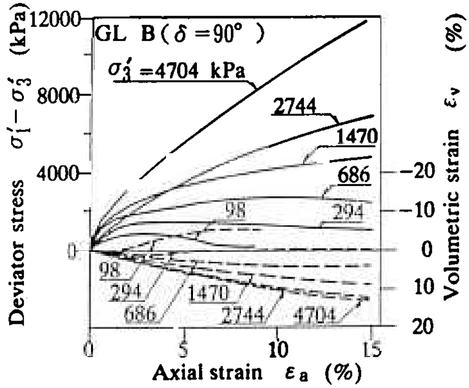

Fig. 2. Deviator stress, volumetric strain–axial strain curves

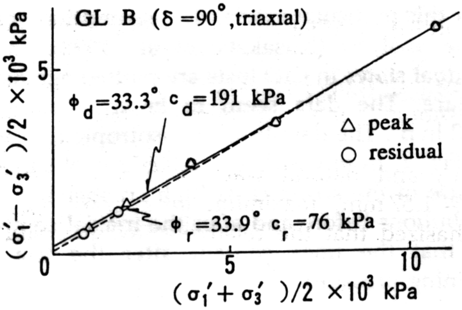

Fig. 3. Failure envelope of Mohr's Circles at failure and residual state

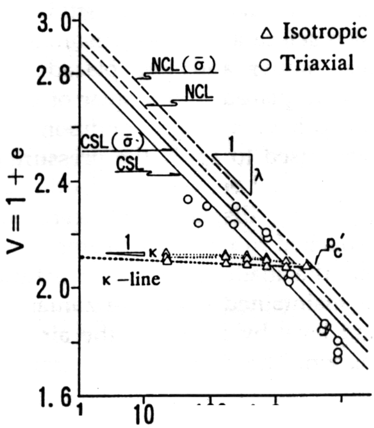

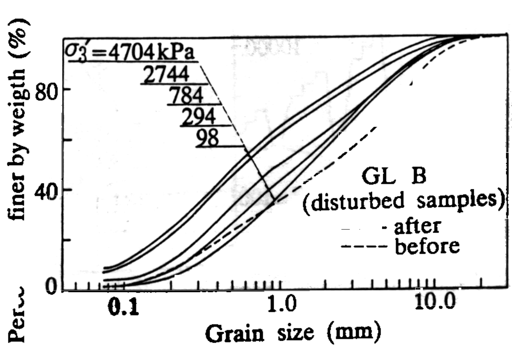

Fig. 5. Change in grain-size distribution curves before and after triaxial tests

showed that for this particular scoria, the assumption of isotropy may be adopted for the analysis (Kusakabe et al., 1992). In Fig. 4 specific volumes at residual states in CID tests are plotted against mean effective stresses at failure. The data seem to lie in a straight line, giving $V = 2.826–0.112 \ln p'$. The data from the isotropic compression tests are also plotted in Fig. 4, from which $\kappa = 0.00573$ is obtained.

Another feature of the scoria is its high crushability. Figure 5 shows grain-size distributions before and after the triaxial compression tests. It clearly shows that the fines content after the test increases with increasing confining pressure.

Loading test programme and test procedures

The in situ loading test programme included eight tests with different dimensions of footings. For this particular study, a 400 mm square footing (B = 400 mm) was selected for comparison. A model footing was composed of rigid steel frames and was placed onto the excavated ground surface after having placed a thin layer of cement paste on the surface ground in order to have a rough condition at the footing base. Four hydraulic jacks were used to apply the pressure onto the footing, and a pin joint was implemented between the footing and the jacks. The measurements of the footing displacement were made at the four corners of the footing attached to reference beams.

In order to carry out the loading test on a saturated ground, the ground water level was maintained at the horizontal surface of the base of the excavated ground level by adjusting the air pressure fed to the base chamber of the caisson. The change in the ground water level was

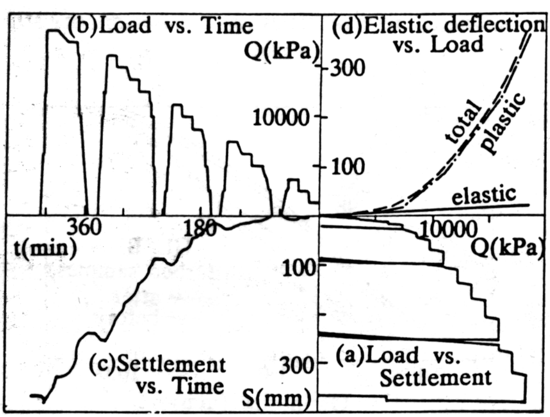

Fig. 6. Loading test results

monitored during the loading test by a float in a small pit dug out in the ground.

The loading was of the load control type, applying the loads in a step loading; at the end of each loading step, the applied force was held constant for 15 min. Prior to the loading test, an elastic consolidation analysis using the CRISP package had been performed with the value of the coefficient of permeability ($k = 3.2 \times 10^{-3}$ cm/s) obtained from in situ permeability tests to ensure that 15 min was sufficient for excess pore water pressure to dissipate and achieve the drained condition. More detailed descriptions and the results of the whole loading tests are reported elsewhere (Kusakabe et al., 1992).

Loading test results

The test results are plotted in Fig. 6, in terms of

(*a*) load (Q) against settlement (S) (Q–S curve)
(*b*) load against time (t) (Q–t curve)
(*c*) settlement against time (S–t curve)
(*d*) load against elastic deflection (recoverable deflection upon unloading) (Se) (Q–Se).

By plotting Q and S in double log-scale the yield load was determined as a deflection point. The ultimate bearing capacity was defined as a point where a linear portion appeared in the Q–S curve plotted in normal scale.

The soils were excavated after the test to investigate failure surfaces. Figure 7 shows a view of the zone beneath the footing after the footing

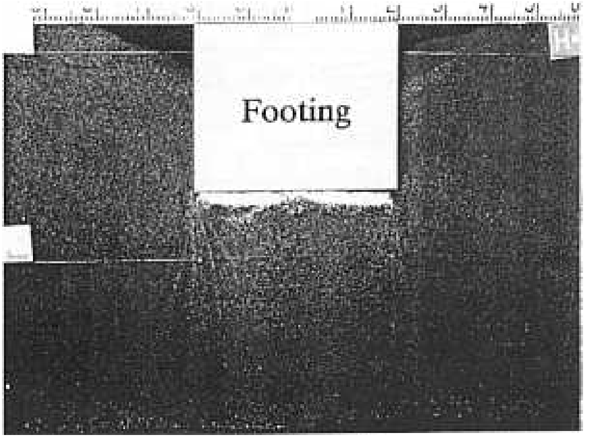

Visible slip lines developed beneath footing was penetrated to an S/B of as large as 0.9, in which the zone beneath the footing is heavily compressed and a series of slip lines developing from both edges of the footing is clearly shown by the change in tone on the excavated surface. Apart from the radial slip lines, no indication of clear shear bands was observed in other zones.

Centrifugal simulation

Centrifuge and test system

Two centrifuge tests with a reduced model (denoted US-2 and US-4) were performed using undisturbed block samples. The centrifuge used was the machine at Utsunomiya University with effective radius 1.18 m. A rectangular strong steel box (inner dimensions 262 mm in width, 299 mm in depth, and 498 mm in length) housed the model ground. The loading system, comprising an AC motor of 0.1 kW, a load cell and a dial gauge, was mounted directly on the strong box. The footing had a concave loading point to simulate the pin condition.

Model preparation and test procedures

The size of model footing was determined to be 1/13.3 of the prototype (30 mm square) by considering that the strong box boundaries do not interfere with possible failure zones. Consequently the centrifugal acceleration was 13.3, giving a prototype footing width (B) of 400 mm. The line of effective radius is located at 1B depth below the ground surface.

Two boxes of the undisturbed samples procured from the B ground

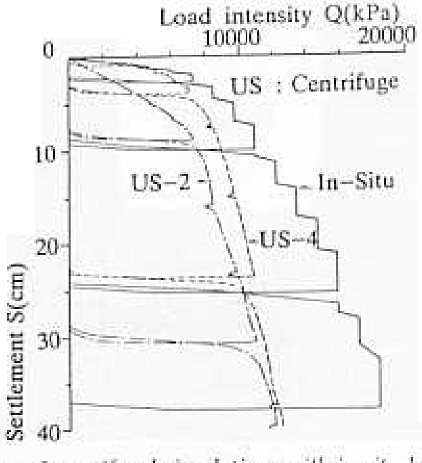

Fig. 8. Comparison of centrifugal simulations with in situ loading test

were used for the centrifuge tests. Model preparation consisted of four stages: water feeding, freezing, trimming and defrosting. Having sprayed water over the undisturbed sample, the sample was kept in a refrigerator at a temperature of −20°C for two days. The block sample was then trimmed down to a size of 180 mm in thickness, 200 mm in width, and 400 mm in length by using the diamond cutter fitted into a wooden liner for handling purposes. The trimmed sample was again placed in the refrigerator for another two days. One day before the loading test, the sample was weighed and its dimensions were measured. The model ground in the liner was lowered carefully into the strong box. A gap between the container and the sample was filled with wet Toyoura sand, which was then compacted to achieve the relative density of over 90%.

After placing cement paste on the surface of the model ground, the model footing made of steel was set on that location to simulate prototype conditions as precisely as possible. Water was then gradually fed to the sample from the bottom of the container for two hours and the container was hung from the centrifuge arm. Water was further added from the top surface of the sample. The centrifuge was accelerated to 13.3 G in 4 min and maintained for 15 min before the loading sequence was started.

Because of the system available at that time, the loading was of the settlement control type and was therefore different from the prototype condition. According to the $1/n^2$ similitude for time, an equivalent rate of loading and unloading of 4 mm/min was adopted and the load holding time was 5 s, corresponding to 15 min in prototype.

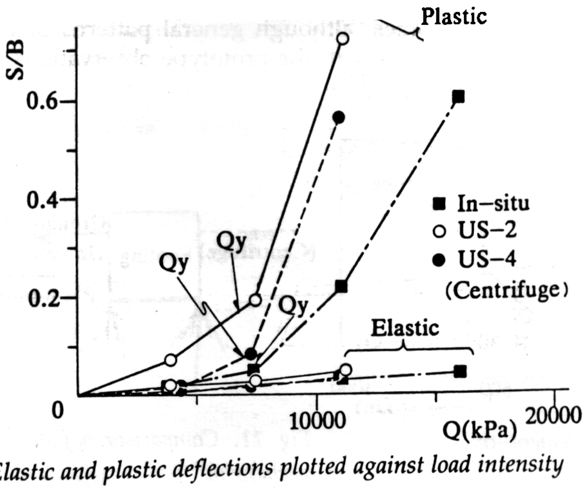

Fig. 9. Elastic and plastic deflections plotted against load intensity

Results of centrifugal simulations and comparisons

The load–intensity settlement curves obtained in the centrifuge tests are superimposed on Fig. 6(*a*), as is presented in Fig. 8. Curves of the two centrifuge tests are somewhat different in the early stage and become very close to each other in the later stage. What is noticeable in direct comparison with the prototype is that the centrifugal simulations underestimate both the coefficient of initial subgrade reaction K_{Vi}, and the yield load intensity Q_y and ultimate bearing capacity Q_u. The ratios of centrifuge result to prototype are 0.98 (US-4), 0.23 (US-2) for K_{Vi}, 0.93 (US-4), 0.89 (US-2) for Q_y, and 0.76 (US-4), 0.68 (US-2) for Q_u, respectively. Here, the determination of the yield load and ultimate load were the same as those adopted in the field test. Similarly, the ratio of centrifuge to prototype about the settlement/footing width ratios (for yield S_y/B; for ultimate S_u/B) are 1.05, 0.80 for the case of US-4.

Figure 9 shows the relationship between the elastic deflection and the load intensity for the case of US-4. It is clear that the centrifugal simulation predicts fairly well the value of elastic deflection even up to beyond the yield loads of the tests, suggesting that the centrifuge tests results in larger plastic deflections.

Settlement controlled loading was used in the centrifuge, whereas the prototype loading tests were of load control type. The match between the centrifuge simulation and prototype in terms of the settlement–time relationship is compared in Fig. 10. It is seen that up to 1.15 times the prototype yield load both are quite close to each other. Large discrepancy after yield would not affect other comparisons, provided that both prototype and centrifuge tests had been conducted under drained conditions.

Figure 11 compares the failure mechanism. Centrifuge models did not exhibit clear visible slip lines, although general patterns of the failure mechanism are in conformity with the prototype observations.

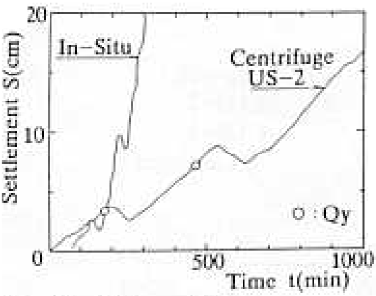

Fig. 10. Settlement–time relationship

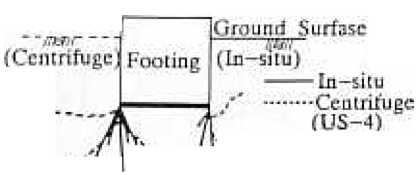

Fig. 11. Comparison of failure mechanism

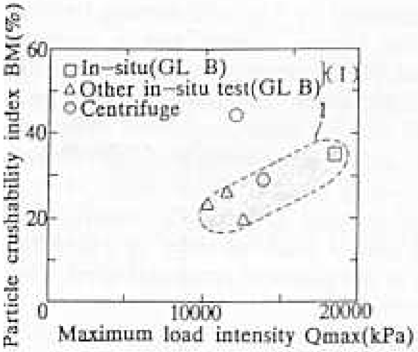

Fig. 12. Particle crushability index versus maximum load intensity

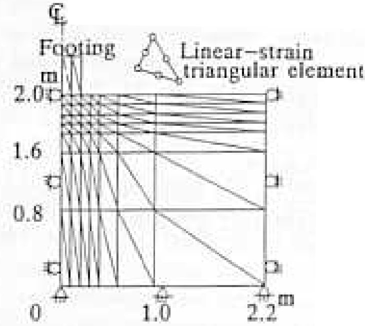

Fig. 13. FEM discretization of loading test

It was pointed out earlier that the scoria has a tendency for particle crushing. Both in the prototype and centrifuge tests, the two grain size distributions were measured after the tests; one from directly beneath the footing and the other from a point away from the loading point. Figure 12 summarizes the results of particle crushing in terms of crushability ratio defined by Marsal (1965), who plotted the crushability ratio against load intensity including the data of three other loading tests conducted on the B ground. There seems a trend that the crushability ratio increases with increasing load intensity. The degree of particle crushing is strongly related to the pressure level that the ground will experience, as is seen in Fig. 12. The centrifuge test does simulate the phenomenon of particle crushing, but the degree of particle crushing is underestimated because of the underestimation of the ultimate bearing capacity.

Numerical simulation

CRISP programme and analysis conditions

The CRISP programme is readily available in Japan with a Japanese user's manual (Akaishi et al., 1989). One of the attractive features of the CRISP programme is that it can be used on a personal computer. The personal computer used for this analysis was a 32-bit NEC PC-H98 S-model with a 100 Mb hard-disk memory.

The original Cam-clay model (Schofield and Wroth, 1964) was purposely selected as a constitutive model. For granular materials, alternative soil models are of course available and analyses with sophisticated constitutive soil models could have been done, but requires a mainframe computer, which was not our intention for this particular study.

The 400 mm square footing was modelled by a circular footing having the same cross-sectional area as the square footing and a drained axisymmetric analysis was carried out. FEM discretization of the loading test is shown in Fig. 13. It has 102 cubic strain triangular elements and 67 nodes. A depth of 5 B and a width of 5.5 B were considered adequate for the purpose of analysis. The boundary conditions of displacement imposed in the analysis are also shown in Fig. 13. It was assumed that the footing is effectively rigid and its base is perfectly rough. The number of loading steps was 1402 with a load intensity of 7415 kPa, which was restricted by the capacity of the personal computer used. The execution time was typically about 18 h.

The necessary input critical state parameters (κ, λ, M, Γ, p_c') were selected mainly from the data of the triaxial CID and the isotropic compression tests. Namely, κ was determined from the rebound portion of the isotropic compression tests. λ was taken from Fig. 4. The value of M was estimated from the residual friction angle of 33.9° from Fig. 3. In order to satisfy the relationship of the Cam clay between the above parameters.

$$N = \Gamma + \lambda - \kappa,$$

the critical state line was shifted to the right by one standard deviation ($\bar{\sigma}$) and then N and Γ values were determined as 2.99, 2.89, respectively. Consequently the p_c' value became 3840 kPa.

Poisson's ratio (ν) was evaluated to be 0.3 from two elastic soil parameters K and G obtained from the initial portions of volumetric strain–deviator stress curve, and deviator strain–stress curves in the CID tests, respectively. The values of relevant soil parameters are summarized in Table 1. The ground water level was set at the ground surface. Initial vertical effective stresses were assumed to be of a trapezoidal shape due to selfweight with a small surcharge of 1 kPa.

Since K_0 values were not measured in situ, three different methods were used to estimate the K_0 values. The process of one-dimensional loading to p_c' value of 3840 kPa and unloading to the in situ effective vertical stress was simulated by a CRISP calculation using the soil parameters listed in Table 1, which gave $K_{nc} = 1.0$ and $K_0 = 17$. Wroth (1975) and Parry (1982) proposed the followed equations for K_0: $K_0 = OCR \times K_{nc} - \{\nu(OCR - 1)/(1 - \nu)\}$,

$$K_0 = K_{nc} \times (OCR)^{\phi'}.$$

Table 1. Soil parameters used in CRISP

κ	λ	Γ	M	ν	γ (kN/m^3)
0.00573	0.112	2.89	1.37	0.3	18.6

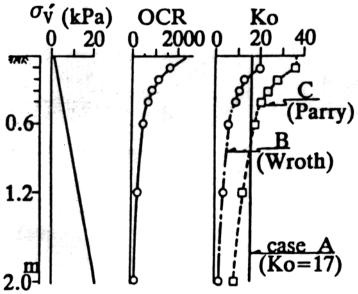

Fig. 14. In situ stress distribution in analysis

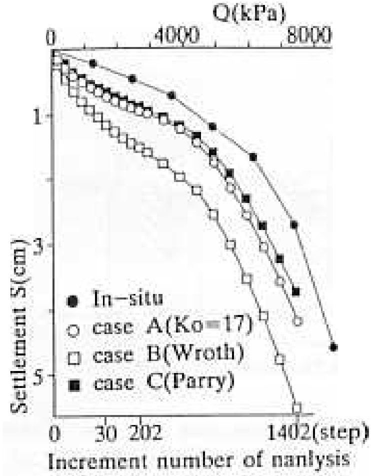

Fig. 15. Comparison of pressure curves for different in situ stress conditions

Using Jaky's equation $K_{nc} = 1 - \sin\ \phi'$ for OCR = 1, the vertical preconsolidation stress was calculated to be 3190 kPa. In situ stress distributions assumed in the analysis are shown in Fig. 14. Note that OCRs are extremely high in the zone shallower than 1B depth; consequently extremely high values of K_0 are obtained. Although these are outside the range of values considered reasonable, it should be mentioned here that none of the effective horizontal stresses calculated by these three methods exceeds the Rankine passive earth pressure using the residual strength parameters.

Results of numerical simulations and comparisons

Figure 15 is a comparison of the load-intensity–settlement curves against the prototype for various K_0 values, which clearly indicates that the shape of the initial portion of the curves is strongly influenced by the selection of K_0 values. The best fit curves up to the yield load among the three are the ones with the K_0 distributions predicted by the CRISP and suggested by Parry, although they overestimate the settlements by a factor of about 1.4 at a prototype load intensity of 7415 kPa.

Development of failure was examined by plotting the three zones (hardening, critical state and softening) at two different loading stages, as shown in Fig. 16(*a*). The slip lines observed in the prototype are also drawn. Figure 15(*b*) presents the state paths of two particular elements, one beneath the footing, the other in the passive zone. It is noted that

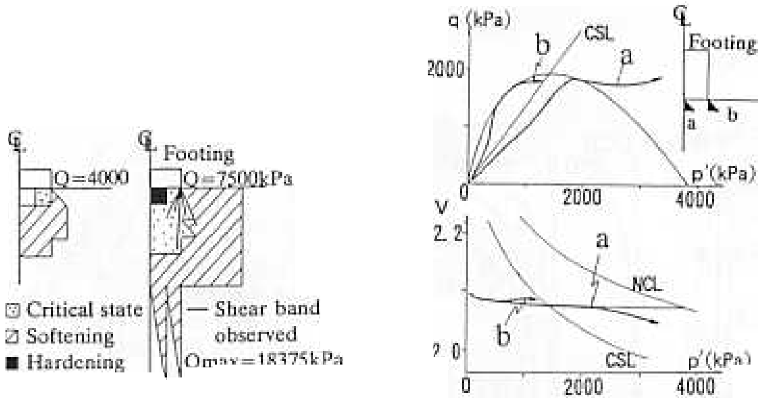

(a)Development of Zone Yielded and Approaching Critical State

(b)State Paths of Subsoils Computed by CRISP

Fig. 16. Plastic zone and state paths

the zone of critical state is well matched with the area where the slip lines were observed, whereas the area beneath the footing is compressed and continuously hardening as is seen in the behaviour of the element (a), suggesting that particle crushing may be probable. This result is in conformity with the observation in the field.

Discussion

The centrifugal simulation carried out in this study was a relatively straightforward exercise, but assumed that the freezing and thawing process provided undisturbed samples of high quality. Although the yield load was quite accurately predicted, the difference between centrifuge and prototype did exist in two aspects:

(1) the underestimation of the coefficient of initial subgrade reaction K_{Vi}, and the ultimate load Q_u, and
(2) the overestimation of plastic settlement.

Both of these may be on-the-safe-side predictions from a practical point of view. The underestimation of K_{Vi}, Q_u may have arisen from the difference in loading system, the disturbance of samples and, in particular, the deterioration of the cohesion term of the cemented scoria. The overestimation of plastic deformation may have resulted from the fact that the ratio of particle size to footing width (B/D_{50}) was as small as 8.82–13.6. This may be compared with the case of the loading tests on Shirasu, of which the B/D_{50} value was about 6 times larger than the above. It is obvious that further research is required into whether centrifuge tests for natural granular deposits give predictions on the safe side or unsafe side, and into how seriously particle size affects the test results of granular materials. But the authors' experience in this attempt was that centrifuge modelling did work well in estimating the bearing capacity and in producing crushing phenomenon.

In FEM simulations some difficulties were experienced, mostly the selection of soil parameters and K_0 value. Some freedom was used to determine values of N and Γ consistent with the Cam clay model, which may imply that the Cam clay may not be the best choice for modelling the scoria dealt with in this study. It was demonstrated that the initial portion of the load–settlement curve was very sensitive to the selection of the K_0 value, and the use of a very high K_0 was needed to get reasonable agreement up to the yield load. This poses two questions:

(*a*) how to select appropriate elastic parameters for modelling the scoria, constant shear modulus G, or K varying with p′, as is the Cam clay model

(*b*) how to estimate K_0 values for extremely high over-consolidation ratios, as is the case of this study.

These are the problems associated with soil model rather than those of numerical scheme.

As to the comparison of the two modellings it must be emphasized that the centrifuge tests readily provided the results without any information about soil element behaviour (best soil model and proper values for parameters) and in situ stress conditions.

Concluding remarks

A series of large-scale loading tests was successfully carried out in a pneumatic caisson which provided a body of information about the prototype behaviour of shallow footing on cemented and structured granular materials susceptible to particle crushing. It was found that centrifugal simulations using undisturbed samples predicted the yield load to be 89–93% of the corresponding prototype, and elastic deformations close to the prototypes. In the models, although the phenomenon of the particle crushing was observed, clear slip lines were not developed and settlements at yield load were larger than those in prototype. It was inferred that the two observations may be partly due to the particle size effect, which requires further research.

Attempts at numerical simulation for a scoria, naturally deposited, cemented granular material were made by the CRISP programme with the Cam clay model. Difficulty in the selection of soil parameters was encountered and the uncertainty in the determination of K_0 values for very high overconsolidation ratios was recognized.

References

Akaishi, M., Kusakabe, O., Kogo, T. and Takagi, N. (1989). CRISP manual, Tokai University Press (in Japanese).

Almeida, M.S.S., Britto, M. and Parry, R.H.G. (1986). Numerial modeling of centrifuged embankment on soft clay. Canadian Geotechnical Journal, Vol. 23, pp. 103–114.

Basset, R.H. and Horner, J. (1979). Prototype deformations from centrifuge model tests. Proc. of 7th European Regional Conf. on SMFE, Vol. 1, pp. 1–9.

Basset, R.H., Davies, M.C.R., Gunn, M.J. and Parry, R.H.G. (1981). Centrifuge models to evaluate numerical methods. Proc. 10th ICSMFE, Vol. 1, pp. 557–562.

Bolton, M.D. and Lau, C.K. (1988). Scale effects arising from particle size, Centrifuge '88, edited by Corte, Balkema, pp. 127–131.

Britto, A.M. and Gunn, M.J. (1987). Critical state soil mechanics via finite elements, Ellis Horwood.

Davies, M.C.R. and Parry, R.H.G. (1985). Centrifuge modelling of embankments on clay foundations, Soils and Foundations, Vol. 25, No. 4, pp. 19–36.

Fujii, N., Kusakabe, O., Keto, H. and Maeda, Y. (1988). Bearing capacity of a footing with an uneven base on slope: Direct comparison of prototype and centrifuge model behaviour, Centrifuge '88, edited by Corte, Balkema, pp. 301–306.

Indraratna, B., Balasubramaniam, A.S. and Balachandran, S. (1992). Performance of test embankment constructed to failure on soft marine clay. ASCE Journal of Geotechnical Engineering, Vol. 118, No. 1, pp. 12–33.

Kimura, T., Kusakabe, O. and Saitoh, K. (1984). Undrained deformation of clay of which strength increases linearly with depth. Proc. of Symp. Application of centrifuge modelling to geotechnical design, pp. 315–335.

Kusakabe, O., Maeda, T., Ohuchi, M. and Hagiwara, T. (1991). Strength-deformation characteristics of an undisturbed scoria and effects of sampling disturbance (in Japanese), Proc. of Japan Society of Civil Engineers. No. 430/III -15, pp. 97–106.

Kusakabe, O., Maeda, Y. and Ohuchi, M. (1992). Large-scale loading tests of shallow footings in a pneumatic caisson. ASCE, Journal of Geotechnical Engineering, Vol. 118, No. 11, pp. 1681–1695.

Lyndon, A and Schofield, A.N. (1970). Centrifugal model test of a short-term failure in London clay, Geotechnique, Vol. 20, 440–442.

Lyndon, A. and Schofield, A.N. (1978). Centrifugal model tests of the Lodalen landslide. Canadian Geotechnical Journal, Vol. 5, pp. 1–13.

Marsal, R.J. (1965). Soil properties–shear strength and consolidation, Proc. 6th Int. Conf. SMFE, Vol. 3, pp. 310–316.

PARRY, R.H.G. (1982). Quoted by Britto and Gunn (1987), p. 184.

SCHOFIELD, A.N. AND WROTH, C.P. (1964). Critical State Soil Mechanics, McGraw-Hill.

TATSUOKA, F., OKAHARA, M., TANAKA, T., TANI, K., MORIMOTO, T. AND SIDDIQUEE, M.S.A. (1991). Progressive failure and particle size effect in bearing capacity of a footing on sand, Geotechnical Engineering Congress, ASCE, Vol. II, pp. 788–802.

WROTH, C.P. (1975). In-situ measurements of initial stresses and deformation characteristics, Proc. Spec. Conf. on In-situ measurement of soil properties, ASCE, pp. 181–230.